

Spectral hole burning and its application in microwave photonics

Stefan Putz^{1,2,3*}, Andreas Angerer^{1,2†}, Dmitry O. Krimer⁴, Ralph Glattauer¹, William J. Munro^{5,6}, Stefan Rotter⁴, Jörg Schmiedmayer^{1,2} and Johannes Majer^{1,2*}

Spectral hole burning, used in inhomogeneously broadened emitters, is a well-established optical¹ technique, with applications from spectroscopy to slow light² and frequency combs³. In microwave photonics⁴, electron spin ensembles^{5,6} are candidates for use as quantum memories⁷ with potentially long storage times⁸. Here, we demonstrate long-lived collective dark states⁹ by spectral hole burning in the microwave regime¹⁰. The coherence time in our hybrid quantum system (nitrogen-vacancy centres strongly coupled to a superconducting microwave cavity) becomes longer than both the ensemble's free-induction decay and the bare cavity dissipation rate. The hybrid quantum system thus performs better than its individual subcomponents. This opens the way for long-lived quantum multimode memories, solid-state microwave frequency combs, spin squeezed states¹¹, optical-to-microwave quantum transducers¹² and novel metamaterials¹³. Beyond these, new cavity quantum electrodynamics experiments will be possible where spin–spin interactions and many-body phenomena¹⁴ are directly accessible.

Quantum information science and metrology rely on the coherent manipulation of two-level systems, which allow the storage of single excitations in high-capacity multimode memories¹⁵. The manipulation of information within those memories has proven to be difficult, and so the hybridization of distinct quantum systems to form quantum metamaterials offers a realistic way forward. Such 'hybrid' quantum systems have become a key strategy in microwave circuit cavity quantum electrodynamics (cQED)^{4,16}. As an example we discuss the hybridization of superconducting devices with electron spin ensembles^{5,6,17} and show their potential to bypass individual weaknesses while harnessing their strengths. Electrical circuits offer easy manipulation and processing^{18,19}, yet have limited coherence properties, while single electron spins in semiconductor crystals can have coherence times of up to almost one hour²⁰ but are hard to manipulate. In early experiments, coherent energy exchange on the single-photon level and basic memory operations⁷ were demonstrated in this context²¹.

An outstanding challenge in solid-state-based hybrid systems is the suppression of spin dephasing induced by the host material^{5,6,17}. However, the realization of true multimode memories is only possible in the presence of inhomogeneous spectral broadening and so their short memory times have to be actively recovered by echo refocusing techniques²¹ or improved by the cavity protection effect²². In this Letter, we present an alternative approach based on collective dark states^{9,23} that circumvents the necessity for recovery protocols and substantially improves the coherence times beyond the limit given by the cavity and spin ensemble.

Our hybrid system consists of a superconducting resonator with a diamond crystal containing an ensemble of negatively charged nitrogen–vacancy (NV) centre electron spins magnetically coupled to it (Fig. 1a,b). The device was placed in a dilution refrigerator operating at temperatures <25 mK. The resonator was characterized at zero external magnetic field by transmission spectroscopy and was determined to have a fundamental resonance at $\omega_c/2\pi = 2.691$ GHz with a cavity linewidth of $\kappa/2\pi = 440 \pm 10$ kHz and quality factor of $Q = 3,130$. The diamond crystal has a NV concentration of $\sim 4 \times 10^{17}$ cm⁻³, meaning that the macroscopic spin ensemble in the cavity mode volume consists of $N \approx 1 \times 10^{12}$ NV spins thermally polarized ($\geq 99\%$) at our refrigerator's base temperature. These electron spins were Zeeman-shifted into resonance with the cavity by applying an external d.c. magnetic field (Fig. 1c).

We observed a mode splitting and Rabi oscillations with frequency $\Omega_R/2\pi = 21.3 \pm 0.1$ MHz and linewidth/decay rate of $\Gamma/2\pi = 1.45 \pm 0.05$ MHz on probing the system with low intensities of $< 1 \times 10^{-6}$ photons per spin in the cavity (Supplementary Fig. 1). Although the single spin–cavity coupling strength, g_j , is rather small ($\lesssim 10$ Hz) (ref. 6), the large number N of weakly dipole-dipole interacting spins allows us to deeply enter the strong coupling regime ($\Omega_R \gg \Gamma \gg \kappa$) with cooperativity $C \approx 26$. Such an ensemble of individual two-level systems coupled to a single-mode cavity is described by the Tavis–Cummings model, which in the rotating wave approximation can be written as

$$\mathcal{H} = \hbar\omega_c a^\dagger a + \frac{\hbar}{2} \sum_{j=1}^N \omega_j \sigma_j^z + \hbar \sum_{j=1}^N g_j [\sigma_j^- a^\dagger + \sigma_j^+ a] \quad (1)$$

with the cavity modes' bosonic creation (annihilation) operators a^\dagger (a) operating at frequency ω_c . The Pauli spin operators $\sigma_j^{\pm,z}$ are associated with the j th spin at frequency ω_j . In such an ensemble of N spins that share a single excitation, we find one super-radiant state²⁴ $|B\rangle = J^+|G\rangle$ and $N - 1$ subradiant states $|S\rangle$, where $J^\pm = (1/\sqrt{\sum_i^N g_i^2}) \sum_j^N g_j \sigma_j^\pm$ is the collective spin operator and $|G\rangle$ the collective spin ground state.

The hybridized polariton modes $|\pm\rangle = (|1\rangle_c|G\rangle_s \pm |0\rangle_c|B\rangle_s)/\sqrt{2}$ are entangled states between the cavity and the super-radiant spin state. The vacuum Rabi splitting²⁵ is due to a collectively enhanced interaction $\Omega_R/2 \approx \Omega = \sqrt{\sum_i^N g_i^2}$ scaling approximately as \sqrt{N} . Subradiant states remain uncoupled and degenerate in the absence of spin broadening. In the presence of inhomogeneous spin broadening, corresponding to a variation of ω_j centred around a central spin frequency ω_s (Fig. 2a(i),b(i) and c(i)), the polariton modes and subradiant states are not entirely decoupled. The inhomogeneous spin broadening of $\gamma_{inh}/2\pi = 4.55$ MHz is the main source

¹Vienna Center for Quantum Science and Technology (VCQ), Atominstitut, TU Wien, Stadionallee 2, 1020 Vienna, Austria. ²Zentrum für Mikro- und Nanostrukturen, TU Wien, Floragasse 7, 1040 Vienna, Austria. ³Department of Physics, Princeton University, Princeton, New Jersey 08544, USA. ⁴Institute for Theoretical Physics, TU Wien, Wiedner Hauptstraße 8-10/136, 1040 Vienna, Austria. ⁵NTT Basic Research Laboratories, 3-1 Morinosato-Wakamiya, Atsugi, Kanagawa 243-0198, Japan. ⁶National Institute of Informatics, 2-1-2 Hitotsubashi, Chiyoda-ku, Tokyo 101-8430, Japan. [†]These authors contributed equally to this work. *e-mail: stef.putz@gmail.com; jmajer@ati.ac.at

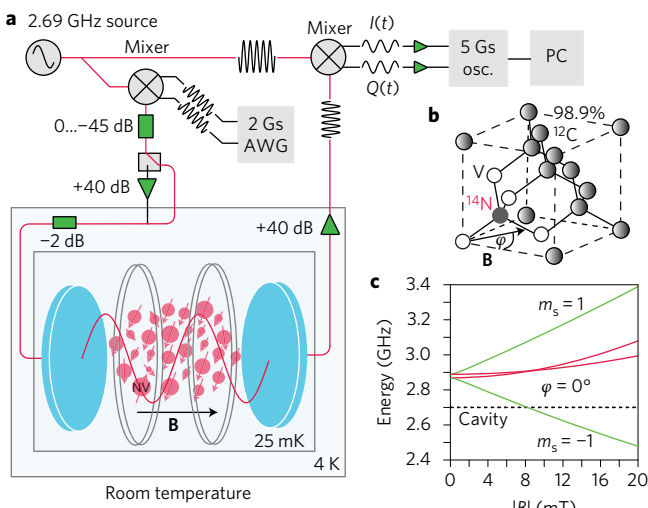


Figure 1 | Experimental set-up. **a**, A superconducting cavity loaded with an enhanced synthetic diamond crystal and surrounded by a three-dimensional d.c. Helmholtz coil cage is placed in a dilution refrigerator operating at temperatures below 25 mK. Further details about the measurement scheme can be found in the Methods. **b**, Structure of the NV defect centre ($S=1$) in diamond consisting of a substitutional nitrogen atom and an adjacent lattice vacancy. **c**, Zeeman tuning of the NV central spin transition frequencies. Red and green indicate the two degenerate NV subensembles.

of decoherence here, accelerating the evolution of an excitation stored in the super-radiant mode into the bath of subradiant states.

The polariton modes $|\pm\rangle$ can be decoupled from the bath of subradiant states by the ‘cavity protection effect’^{26,27}. Only in the limit of $\Omega \rightarrow \infty$ is the decay rate ultimately bound by the mean of both dissipation rates $\Gamma_{\min} = (\kappa + \gamma)/2$. As suggested in ref. 10, it is possible to break this limit of Γ_{\min} by engineering polariton modes that live mostly in the spins, for which the decay rate is much smaller than that of our cavity interface, $\gamma \ll \kappa$. In traditional hole burning, such a long-lived spin population is pumped back into the created hole. Here, however, the strong cavity spin interaction automatically hybridizes a narrow state in the centre of the created spectral hole. We identify the resulting long-lived spin states as ‘collective dark states’^{9,27}, which allows us to improve the total coherence times by over more than one order of magnitude.

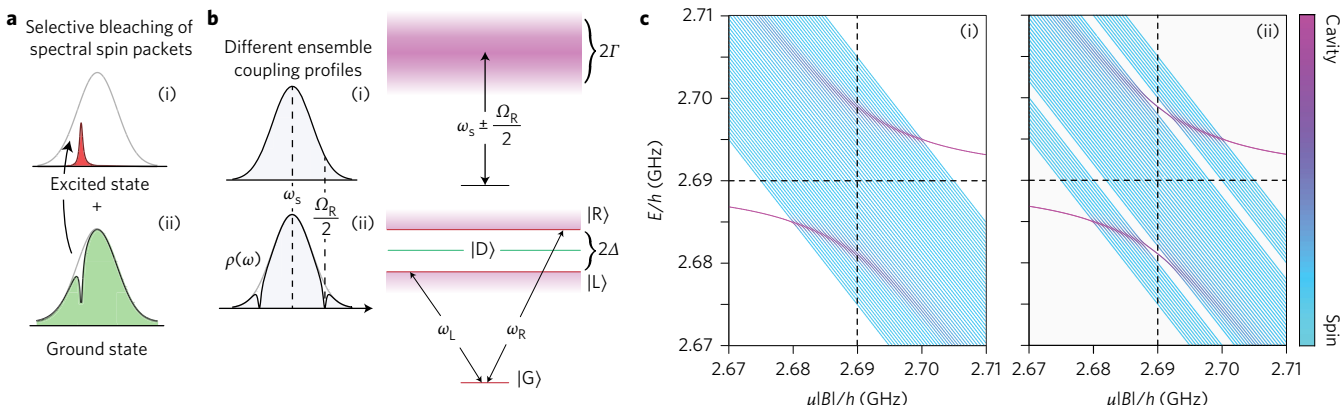


Figure 2 | Visualization of engineered collective dark states. **a**, Spectral hole burning in narrow frequency windows bleaches spin components by bringing them into a mixture between their ground and excited states. The spin density $\rho(\omega)$ (i) is modified (ii). **b**, Two polariton modes of width 2Γ are created in the strong coupling regime ($\Omega_R > 2\Gamma$) (i). If a spin population is removed in a window $\Delta < \Gamma$, the cavity sees a V level system with states $|G\rangle$, $|R\rangle$ and $|L\rangle$ featuring a dark state $|D\rangle$ (ii). **c**, The eigenenergy spectra of the cavity strongly coupled to a broadened spin ensemble with cavity and spin contributions indicated by the colour gradient (colour bar on the right). (i) Two polariton modes in a bath of subradiant states are visible. (ii) Spectral hole burning at $\omega_s \pm \Omega_R/2$ creates long-lived dark states $|D\rangle$, which lie within the created holes and decouple from the remaining bath of subradiant states.

If a hole is burnt at the positions of the polariton modes $\omega_s \pm \Omega_R/2$ (Fig. 2a(ii), b(ii) and c(ii)) two new spin distributions are effectively created left ($|L\rangle$) and right ($|R\rangle$) detuned of the spectral hole. These spin packets share a common ground state $|G\rangle$, meaning that the cavity sees a V level system²⁸ that naturally features a dark state $|D\rangle$. Both transitions $|G\rangle \rightarrow |L\rangle$ and $|G\rangle \rightarrow |R\rangle$ are coupled to the cavity field, and so a small cavity $|1\rangle_c$ component is added to the emerging dark state. If the spectral hole is created in the centre of the polariton mode this dark state

$$|D\rangle \approx \frac{1}{\sqrt{\Delta^2 + 2g_\mu^2}} [g_\mu(|R\rangle - |L\rangle)|0\rangle_c + \Delta|G\rangle|1\rangle_c]$$

lies right in the middle of the spectral hole and is isolated from the bath of subradiant states, with the spectral hole having width Δ and an effective cavity spin coupling strength g_μ . This anti-symmetric long-lived spin state $|D\rangle$ has a linewidth $\Gamma_D \geq \gamma$, which is governed by the width of the spectral hole Δ and can be substantially narrower than the cavity linewidth κ , as we show in the following.

We created dark states, as shown in Fig. 2a(ii), b(ii) and c(ii), by burning two spectral holes at $\omega_s \pm \Omega_R/2$ with a bandwidth of $\Delta/2\pi = 235$ kHz (see Methods). This bleaching thermalizes spins into an equal mixture of their ground and excited states and so cancels out their collective spin–cavity interaction. Saturated spins will decay slowly towards their ground state on a timescale of ≥ 10 ms, given by their spin lifetime⁶ of $T_1 = 45$ s, which is shortened due to the Purcell effect²⁹ and spin diffusion resulting from spin–spin interactions. When the hole burning pulse intensity is above a certain power threshold, long-lived dark states are created (Fig. 3a, inset). This shows through long-lived coherent Rabi oscillations after we switch off a strong hole burning pulse (shown in Fig. 3a,b). In Fig. 3c we demonstrate that the hole burning procedure not only suppresses the decoherence but also allows us to control the Rabi flopping frequency when varying the position of the spectral holes.

The achieved decay rates of the engineered collective dark states $\Gamma_D/2\pi = 125 \pm 10$ kHz (Fig. 3a) are significantly below the fundamental limit ($\Gamma_{\min} = (\kappa + \gamma)/2 > 2\pi \times 220$ kHz) reachable by the ‘cavity protection effect’²². As a result of the created spectral holes, two narrow peaks emerge directly on top of the polariton modes. To observe this directly, we compared the spectrally transmitted steady-state intensity $|A(\omega_p)|^2$, as depicted in Fig. 3d, before and

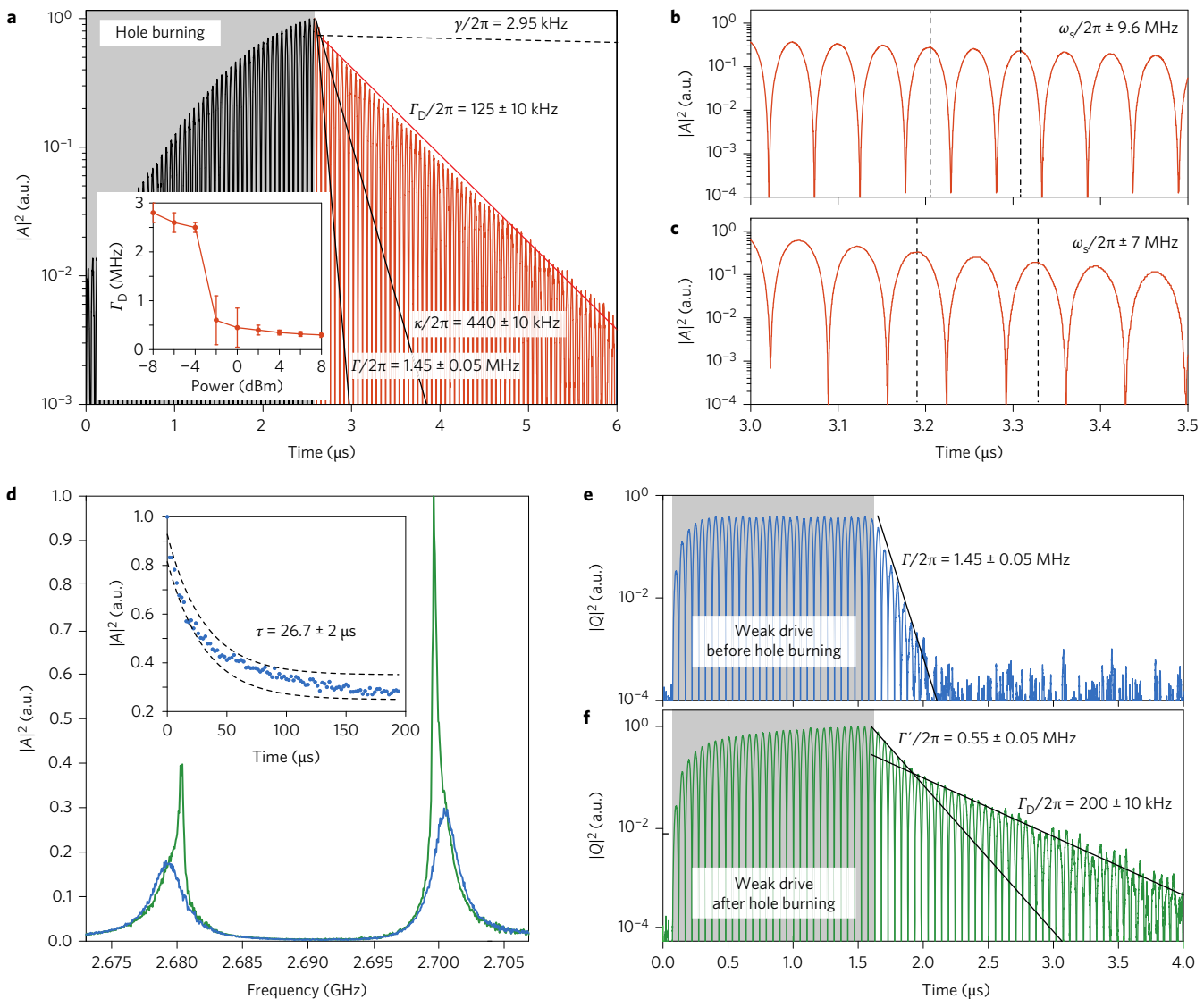


Figure 3 | Spectral hole burning, dark state spectroscopy and dark state dynamics. **a**, Two spectral holes are burned at $\omega_s/2\pi \pm 9.6$ MHz with a bandwidth $\Delta/2\pi = 235$ kHz. When the hole burning pulse intensity reaches a critical threshold (inset), the decay rate is slowed after the drive is switched off (red). **b**, Close-up of the damped Rabi oscillations shown in **a**. **c**, The Rabi frequency is controlled by changing the position of the spectral holes. **d**, The spectral transmitted steady-state intensity through the cavity is scanned with weak probe powers: before (blue) and >5 μ s after (green) a hole burning pulse has decayed. Two narrow peaks emerge directly on top of the polariton modes, identified as the created dark states. The unequal peak amplitudes are caused by an additional Fano resonance, although spins and cavity are in resonance ($\omega_c = \omega_s$). The lifetime of the holes is measured by repeatedly probing the system with low intensities and monitoring the decaying dark-state amplitude (inset). **e**, Linear dynamical response for a sinusoidally modulated weak pulse (grey area, see Methods). **f**, The substantially improved coherence time is shown by probing the system as in **e**, but 5 μ s after spectral holes were burnt and the cavity was emptied. Errors in **a–f** correspond to the minimum and maximum values of the estimated decay rates and in the inset of **d** to the 1σ deviation.

after spectral holes were burnt at positions equal to $\omega_s \pm \Omega_R/2$. The created holes and engineered dark states in Fig. 3d decay with a time constant $\tau = 26.7 \pm 2$ μ s due to spin diffusion, which limits the spectral hole lifetime. In our experiment this is more than four times longer than the best achievable spin echo time $T_2 = 4.8 \pm 1.6$ μ s. We conclude that $\tau \sim 1/2\gamma$, as both rates are limited by spin diffusion in our experiment (see Methods).

It is possible to use this procedure to store and retrieve a weak intensity excitation from the spin ensemble. We drove our system with a weak ($<1 \times 10^{-5}$ photons per spin) sinusoidally modulated pulse. In the absence of spectral holes we observed the unchanged system decay rate $\Gamma/2\pi = 1.45 \pm 0.05$ MHz after switching off the driving tone (Fig. 3e). We then applied a hole burning pulse and, 5 μ s after the signal has decayed, the system was probed again. After the weak probe pulse was switched off, different decay rates

were clearly distinguishable in the Rabi oscillations (Fig. 3f). We first observed a reduced decay rate, $\Gamma'/2\pi = 550 \pm 50$ kHz, due to the created spectral holes and reduced damping of the bright polariton modes. This first decay was followed by a crossover to a second much slower decay, $\Gamma_D/2\pi = 200 \pm 10$ kHz, featuring long-lived Rabi oscillations as the hallmark of the created dark states.

To show the potential of this hole burning we created multiple pairs of dark states. Four spectral holes were created in the polariton modes with $\Delta/2\pi = 150$ kHz bandwidth at positions $\nu_1^\pm = \omega_s/2\pi \pm 9$ MHz and $\nu_2^\pm = \omega_s/2\pi \pm 10.8$ MHz. In Fig. 4 we probe the dynamical response after the hole burning with a weak sinusoidally modulated microwave pulse and observe a clear beating in the Rabi oscillations with a mean dark state decay rate of $\Gamma_D/2\pi = 280 \pm 20$ kHz. The beat frequency of ~ 1.8 MHz corresponds to the frequency difference of both spectral holes in each polariton mode. The two revivals in the Rabi oscillations

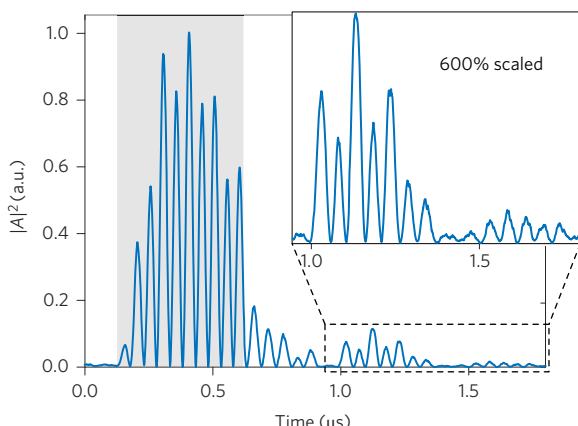


Figure 4 | Engineering of multiple dark states. We create four spectral holes and dark states at frequencies $\nu_1^\pm = \omega_s/2\pi \pm 9$ MHz and $\nu_2^\pm = \omega_s/2\pi \pm 10.8$ MHz close to the polariton modes. The response is probed with weak pulse intensities of $\sim 1 \times 10^{-5}$ photons per spin in the cavity. After the sinusoidally modulated drive with frequency $\Omega_R/2$ and carrier frequency $\omega_p = \omega_c = \omega_s$ (grey area) is switched off, we observe a clear beating with $\Delta_{\nu_{21}} \approx 1.8$ MHz characterized by revivals of the damped Rabi oscillations decaying with a rate $\Gamma_D/2\pi = 280 \pm 20$ kHz. Error corresponds to the minimum and maximum values of the estimated decay rate.

are a clear signature of the coherent dark states beating against each other. This is a first step towards the realization of a solid-state microwave frequency comb, in which one could ideally address up to approximately T/Δ long-lived dark states in one polariton mode.

To conclude, we have demonstrated how spectral hole burning can be used to selectively bleach the ensemble's absorption spectrum in the microwave domain. The created holes allow the engineering of coherent collective long-lived dark states that decay significantly more slowly than the constituent subsystems. This hybridizes the system in such a way that the overall coherence time is no longer bound by the cavity and spin ensemble linewidth. Our work can be seen as a first proof-of-principle experiment for the great potential of hybrid systems. The reported technique opens new possibilities in quantum devices and a new class of cavity QED experiments beyond the standard Dicke²⁴ and Tavis–Cummings model.

Methods

Methods and any associated references are available in the [online version of the paper](#).

Received 28 May 2016; accepted 10 October 2016;
published online 21 November 2016

References

- Moerner, W. E. *Persistent Spectral Hole-Burning: Science and Applications* (Springer Science & Business Media, 2012).
- Turukhin, A. V. *et al.* Observation of ultraslow and stored light pulses in a solid. *Phys. Rev. Lett.* **88**, 023602 (2001).
- de Riedmatten, H., Afzelius, M., Staudt, M. U., Simon, C. & Gisin, N. A solid-state light-matter interface at the single-photon level. *Nature* **456**, 773–777 (2008).
- Xiang, Z.-L., Ashhab, S., You, J. Q. & Nori, F. Hybrid quantum circuits: superconducting circuits interacting with other quantum systems. *Rev. Mod. Phys.* **85**, 623–653 (2013).
- Kubo, Y. *et al.* Strong coupling of a spin ensemble to a superconducting resonator. *Phys. Rev. Lett.* **105**, 140502 (2010).
- Amsüss, R. *et al.* Cavity QED with magnetically coupled collective spin states. *Phys. Rev. Lett.* **107**, 060502 (2011).

- Nunn, J. *et al.* Multimode memories in atomic ensembles. *Phys. Rev. Lett.* **101**, 260502 (2008).
- Plankensteiner, D., Ostermann, L., Ritsch, H. & Genes, C. Selective protected state preparation of coupled dissipative quantum emitters. *Sci. Rep.* **5**, 16231 (2015).
- Zhu, X. *et al.* Observation of dark states in a superconductor diamond quantum hybrid system. *Nat. Commun.* **5**, 3424 (2014).
- Krimer, D. O., Hartl, B. & Rotter, S. Hybrid quantum systems with collectively coupled spin states: suppression of decoherence through spectral hole burning. *Phys. Rev. Lett.* **115**, 033601 (2015).
- Wineland, D. J., Bollinger, J. J., Itano, W. M. & Heinzen, D. J. Squeezed atomic states and projection noise in spectroscopy. *Phys. Rev. A* **50**, 67–88 (1994).
- Stannig, K., Rabl, P., Sørensen, A. S., Zoller, P. & Lukin, M. D. Optomechanical transducers for long-distance quantum communication. *Phys. Rev. Lett.* **105**, 220501 (2010).
- Rakhmanov, A. L., Zagorskin, A. M., Savel'ev, S. & Nori, F. Quantum metamaterials: electromagnetic waves in a Josephson qubit line. *Phys. Rev. B* **77**, 144507 (2008).
- Ma, W.-L. *et al.* Uncovering many-body correlations in nanoscale nuclear spin baths by central spin decoherence. *Nat. Commun.* **5**, 4822 (2014).
- Lvovsky, A. I., Sanders, B. C. & Tittel, W. Optical quantum memory. *Nat. Photon.* **3**, 706–714 (2009).
- İmamoğlu, A. Cavity QED based on collective magnetic dipole coupling: spin ensembles as hybrid two-level systems. *Phys. Rev. Lett.* **102**, 083602 (2009).
- Schuster, D. I. *et al.* High-cooperativity coupling of electron–spin ensembles to superconducting cavities. *Phys. Rev. Lett.* **105**, 140501 (2010).
- Nakamura, Y., Pashkin, Y. A. & Tsai, J. S. Coherent control of macroscopic quantum states in a single-Cooper-pair box. *Nature* **398**, 786–788 (1999).
- Wallraff, A. *et al.* Strong coupling of a single photon to a superconducting qubit using circuit quantum electrodynamics. *Nature* **431**, 162–167 (2004).
- Saeedi, K. *et al.* Room-temperature quantum bit storage exceeding 39 minutes using ionized donors in silicon-28. *Science* **342**, 830–833 (2013).
- Wu, H. *et al.* Storage of multiple coherent microwave excitations in an electron spin ensemble. *Phys. Rev. Lett.* **105**, 140503 (2010).
- Putz, S. *et al.* Protecting a spin ensemble against decoherence in the strong-coupling regime of cavity QED. *Nat. Phys.* **10**, 720–724 (2014).
- Zhang, X. *et al.* Magnon dark modes and gradient memory. *Nat. Commun.* **6**, 8914 (2015).
- Dicke, R. H. Coherence in spontaneous radiation processes. *Phys. Rev.* **93**, 99–110 (1954).
- Thompson, R. J., Rempe, G. & Kimble, H. J. Observation of normal-mode splitting for an atom in an optical cavity. *Phys. Rev. Lett.* **68**, 1132–1135 (1992).
- Kurucz, Z., Wesenberg, J. H. & Mølmer, K. Spectroscopic properties of inhomogeneously broadened spin ensembles in a cavity. *Phys. Rev. A* **83**, 053852 (2011).
- Diniz, I. *et al.* Strongly coupling a cavity to inhomogeneous ensembles of emitters: potential for long-lived solid-state quantum memories. *Phys. Rev. A* **84**, 063810 (2011).
- Fleischhauer, M., İmamoğlu, A. & Marangos, J. P. Electromagnetically induced transparency: optics in coherent media. *Rev. Mod. Phys.* **77**, 633–673 (2005).
- Purcell, E. M. Spontaneous emission probabilities at radio frequencies. *Phys. Rev.* **69**, 681 (1946).

Acknowledgements

The authors thank A. Ardavan, B. Hartl, G. Kirchmair, K. Nemoto, H. Ritsch and M. Trupke for helpful discussions. The experimental effort led by J.M. was supported by the Top-/Anschubfinanzierung grant of TU Wien. S.P. and A.A. acknowledge support from the Austrian Science Fund (FWF) in the framework of the Doctoral School 'Building Solids for Function' Project W1243. D.O.K. and S.R. acknowledge funding by the Austrian Science Fund (FWF) through the Spezialforschungsbereich (SFB) NextLite Project No. F49-P10.

Author contributions

S.P., A.A., J.S. and J.M. designed and set up the experiment. A.A. and R.G. carried out the measurements under the supervision of S.P. and J.M. D.O.K. and S.R. devised the theoretical framework and, together with W.J.M., provided the theoretical support for modelling the experiment. S.P. wrote the manuscript and all authors suggested improvements.

Additional information

Supplementary information is available in the [online version of the paper](#). Reprints and permissions information is available online at www.nature.com/reprints. Correspondence and requests for materials should be addressed to S.P. and J.M.

Competing financial interests

The authors declare no competing financial interests.

Methods

The microwave cavity was loaded by placing the diamond sample on top of a $\lambda/2$ transmission line resonator. The superconducting microwave cavity was fabricated by optical lithography and reactive-ion etching of a 200-nm-thick niobium film sputtered on a 330- μm -thick sapphire substrate. The loaded chip was hosted and bonded to a printed circuit board enclosed in a copper sarcophagus and connected to microwave transmission lines.

The spin ensemble was realized by enhancing a type Ib high-pressure high-temperature diamond (HIPHT) crystal containing an initial concentration of 200 ppm nitrogen with a natural abundance of ^{13}C nuclear isotopes. We achieved a total density of ~ 6 ppm negatively charged NV centres by 50 h of neutron irradiation with a fluence of $5 \times 10^{17} \text{ cm}^{-2}$ and annealing the crystal for 3 h at 900 °C. In our system, excess nitrogen P1 centres ($S = 1/2$), uncharged NV⁰ centres, plus additional lattice stress served as the main sources of decoherence and caused spectral line broadening, which by far exceeded dephasing due to the naturally abundant 1.1% ^{13}C spin bath. The characteristics of the diamond crystal and NV ensemble were initially determined at room temperature using an optical laser scanning microscope³⁰. In the present experiment, the broadened spin ensemble was characterized by a q -Gaussian spectral line shape $\rho(\omega)$ with a linewidth of $\gamma_{\text{inh}}/2\pi = 4.55 \text{ MHz}$ (ref. 22).

The negatively charged NV centre is a paramagnetic impurity with electron spin $S = 1$ that consists of a substitutional nitrogen atom and an adjacent vacancy in the diamond lattice. The electron spin triplet can be described by the Hamiltonian, $\mathcal{H}/\hbar = DS_z^2 + \mu BS$, with $\mu = 28 \text{ MHz mT}^{-1}$ and a large zero-field splitting of $D = 2.877 \text{ GHz}$ corresponding to $hD/k_B \approx 138 \text{ mK}$. This allowed us to thermally polarize the NV spin (at finite temperatures of 25 mK) up to 99%. Due to the diamond lattice structure, four different orientations of the adjacent vacancy were possible, resulting in four NV sub-ensembles. Magnetic field strengths on the order of $|B| = 8 \text{ mT}$, applied in the (100) crystallographic plane and parallel to the transmission line resonator, were sufficient to bring the cavity and spins into resonance. In the experiments presented in the main text the magnetic field was rotated by 45° in this plane, at which only two sub-ensembles were degenerate, being in resonance with the cavity.

The measurement scheme was an autodyne detection scheme for spectral hole burning and for measuring the transmitted intensity $|A(t)|^2$ through the cavity. The signal of a microwave source was split into two paths: one serving as cavity probe tone and the other as a local oscillator, both with frequency ω_p . The cavity probe tone was modulated by a frequency mixer and an arbitrary waveform generator (AWG) with 2 GS s⁻¹ sampling frequency. The pulsed microwave probe tone could be attenuated up to -45 dB and routed through a high-power amplifier with $+40 \text{ dB}$ gain by a fast microwave switch. The microwave drive was then fed into the cryostat and attenuated by -2 dB on the 4 K stage, allowing the application of up to 500 mW

power at the cavity input. The transmitted signal was fed into a low-noise amplifier with $+40 \text{ dB}$ gain on the 4 K stage and mixed with the reference signal, and both quadrature signals were recorded by an oscilloscope with 5 GS s⁻¹ sampling frequency. From the measured quadratures $I(t)$ and $Q(t)$, the transmitted microwave intensity $|A(t)|^2$ was calculated (and plotted in Figs 3 and 4 and Supplementary Fig. 2). The transmitted intensity through the cavity resulted in a steady-state signal of $|A|^2 = 5 \times 10^{-4} \pm 2.5 \times 10^{-7} (\text{V}^2)$ for a single shot, which was then averaged 100 times for the measurements shown in Fig. 3e,f (where only one quadrature $|Q|$ is plotted) and Fig. 4. All line- and bandwidths and associated decay rates are given as half-width at half-maximum (HWHM).

Hole burning was experimentally achieved by quadrature amplitude modulation of a high-intensity hole burning pulse. The carrier frequency $\omega_p = \omega_c = \omega_s$ was modulated by a sinusoidal signal $\eta_0 \sin(\Omega_R t/2)e^{-i\omega_p t}$ with a Gaussian envelope and bandwidth Δ . Power values of up to $|\eta_0|^2 \propto 20 \text{ mW}$ were obtained, corresponding to a steady state with $\sim 1 \times 10^4$ photons per spin in the cavity. This intensity is strong enough to bleach spin components selectively at the frequencies of the modulated drive signal. Such a pulse creates two frequency components and spectral holes at $\omega_p \pm \Omega_R/2$ with Δ bandwidth. However, the large number of spins in the experiment makes it necessary to use even larger input powers to burn multiple spectral holes in one shot. We therefore used two consecutive $\sim 5\text{-}\mu\text{s}$ -long sequences to create two pairs of holes close to the polaritonic modes. After the creation of single and multiple pairs of dark states we probed the system again with a weak pulse $\eta_0 \sin(\Omega_R t/2)e^{-i\omega_p t}$ ($\omega_p = \omega_c = \omega_s$) corresponding to $< 1 \times 10^{-5}$ photons per spin in the cavity after the hole burning pulse had decayed.

Spin echo spectroscopy measurements were used to quantify the spectral hole lifetime. A Car-Purcell-Meiboom-Gill (CPMG) sequence was used to estimate the spin-spin relaxation time (T_2), and stimulated echo spectroscopy techniques were used to measure the spin-lattice relaxation time in the rotating frame ($T_{1\rho}$). The best achievable echo times in our experiment were $T_2 = 4.8 \pm 1.6 \text{ }\mu\text{s}$ and $T_{1\rho} = 6.4 \pm 0.59 \text{ }\mu\text{s}$, measured by CPMG and stimulated echo, respectively. We therefore conclude that the spin dissipation rate $\gamma \equiv 1/\tau = 2\pi \times 5.9 \text{ kHz}$ is dominated by spin diffusion in our experiment, given that $T_2 \approx T_{1\rho}$. Although limited by the same process, the spectral hole lifetime is more than a factor of four longer than T_2 and $T_{1\rho}$. This can be explained by the misalignment of the external d.c. magnetic field with respect to the NV axis and a bath of excess electron and nuclear spins in the host material.

References

30. Nöbauer, T. *et al.* Creation of ensembles of nitrogen-vacancy centers in diamond by neutron and electron irradiation. Preprint at <http://lanl.arxiv.org/abs/1309.0453v1> (2013).